

Extremum seeking control using a partial sum of input-output product

Jietae Lee^{*,†} and Kwang Soon Lee^{**}

^{*}Department of Chemical Engineering, Kyungpook National University, Daegu 41566, Korea

^{**}Department of Chemical Biomolecular Engineering, Sogang University, Seoul 04107, Korea

(Received 22 February 2016 • accepted 5 August 2016)

Abstract—Recent extremum seeking control that uses a continuous perturbation and the integral feedback of perturbation-output product is based on a static nonlinear process. The method can be applied to dynamic nonlinear processes for tracking and maintaining the optimal operating points. It has several tuning parameters, such as the integral controller gain and the magnitude and frequency of the continuous perturbation signal. The frequency of the continuous perturbation signal should be low enough to ensure the time-scale separation between the real-time optimization and the process dynamics for the closed-loop stability. However, for some processes, fast perturbations are preferred because they can be attenuated easily in subsequent processes such as buffers and storages. For this, we propose an extremum seeking control method where the partial sum of perturbation-output product is used for a faster square-wave perturbation. Simulations for two processes of parallel competing reactions have been given, and a simple liquid level system to test extremum seeking control methods is suggested.

Keywords: Extremum Seeking Control, Square-wave Perturbation, Real-time Optimization, Input Multiplicity

INTRODUCTION

Real-time optimization to track and maintain the optimum operating point is one of the process control objectives as important as regulatory control and has long been studied. It can be accomplished in the optimization level in the process operation hierarchy [1]. The self-optimizing control is to find a set of controller variables whose constant set points lead to near optimal operations indirectly [2]. For the real-time optimization, numerical programming methods can be applied with steady state operations by applying perturbations and waiting [3,4]. These methods may require much time to reach the optimal operation points due to steady state operations. Some use adaptive control methods that identify nonlinear dynamic models and find their optimal points [5,6]. Identification of nonlinear dynamic models can be complex and need several requirements for convergence. Some use sliding mode methods that find and maintain the optimal operating points, relieving disadvantages of the adaptive control methods [7,8].

Methods named extremum seeking (ES) control use continuous perturbations (sinusoidal waves) and averaging. The average of output multiplied by the perturbation signal has process steady state gain information and integral controller drive the process for the steady state gain to be zero, the optimal operating point. Since convergence of ES control methods has been proved [9,10], many studies and applications have been presented [11]. Advantages and limitations are given in [12]. Improvements and modifications have been in progress [13,14]. The ES control methods have been applied in various processes including chemical and biological processes

[15,16].

One of the advantages of ES control methods is their simplicity. Here the ES control method is considered. The ES control method has several tuning parameters, such as the integral controller gain and the magnitude and frequency of a continuous perturbation signal. The frequency of continuous perturbation signal should be low enough to ensure the time-scale separation between the real-time optimization and the process dynamics for the closed-loop stability. However, for some processes, fast perturbations are preferred because they can be attenuated easily in subsequent processes. For this, we propose an ES control method where the partial sum of perturbation-output product is used for the faster perturbation. To illustrate the proposed ES control method, simulations for two processes of parallel competing reactions have been given and a simple liquid level system to test ES control methods is suggested.

EXTREMUM SEEKING CONTROL

Consider a nonlinear dynamical system,

$$\begin{aligned}\dot{x} &= f(x, u) \\ y &= h(x)\end{aligned}\tag{1}$$

Here x is the state vector, u and y are the scalar input and output variables, respectively. For a constant input $u = \bar{u}$, the corresponding state variable \bar{x} and the output \bar{y} at a steady state are given as

$$\begin{aligned}f(\bar{x}, \bar{u}) &= 0 \\ \bar{y} &= h(\bar{x}) = g(\bar{u})\end{aligned}\tag{2}$$

The steady state input-output map $g(\cdot)$ is assumed to have an optimum point, and the extremum seeking (ES) control finds the optimum point $\bar{u} = \bar{u}_{opt}$ such that

[†]To whom correspondence should be addressed.

E-mail: jtlee@knu.ac.kr

Copyright by The Korean Institute of Chemical Engineers.

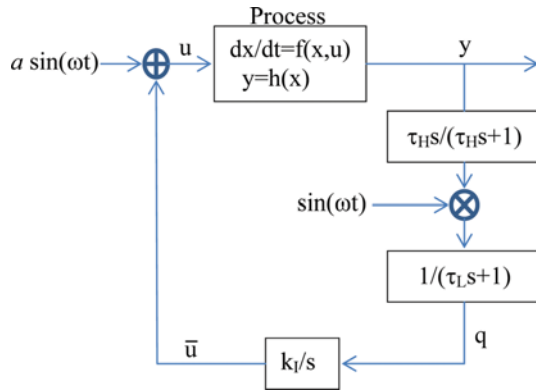


Fig. 1. Original extremum seeking control system.

$$k_p(\bar{u}) = \frac{dg}{d\bar{u}} = 0 \text{ when } \bar{u} = \bar{u}_{opt} \quad (3)$$

The ES control realizes this control task via

$$\begin{aligned} u &= \bar{u} + a \sin(\omega t) \\ q(t) &= y(t) \cdot \sin(\omega t) \\ \bar{u} &= k_I \int_0^t q(t) dt \end{aligned} \quad (4)$$

In applying the ES controller of Eq. (4), for improved transient, high-pass and low-pass filters can be added before and after $q(t)$, respectively, as shown in Fig. 1.

Response of the controller in Eq. (4) can be explained briefly through the two-time scale analysis. Assume that the nonlinear system of Eq. (1) can be linearized as, for a small perturbation of u from \bar{u} ,

$$\begin{aligned} G(s) &= c(sI - A)^{-1}b \\ A &= \frac{\partial f}{\partial x} \Big|_{\bar{x}, \bar{u}}, \quad b = \frac{\partial f}{\partial u} \Big|_{\bar{x}, \bar{u}}, \quad c = \frac{\partial h}{\partial x} \Big|_{\bar{x}} \end{aligned} \quad (5)$$

where $G(s)$ is the process transfer function between the input u and the output y . When the integral gain k_I is sufficiently small, $\bar{u}(t)$ is slowly varying compared to $x(t)$ and $\sin(\omega t)$. The fast subsystem of this two-time scale system becomes

$$\begin{aligned} \dot{x} &= f(x, \bar{u} + a \sin(\omega t)) \\ y &= h(x) \end{aligned} \quad (6)$$

When the excitation size a is small, the output after some time elapses becomes

$$y(t) \cong g(\bar{u}) + k_p a |G(j\omega)| \sin(\omega t - \phi(\omega)) \quad (7)$$

where $\phi(\omega) = \angle G(j\omega)$. The average value of $q(t)$ is

$$\begin{aligned} \bar{q}(t) &= \frac{1}{p} \int_{t-p}^t y(\tau) \sin(\omega \tau) d\tau \\ &\cong k_p \left(\frac{a |G(j\omega)|}{p} \right) \int_{t-p}^t \sin(\omega \tau) \sin(\omega \tau - \phi(\omega)) d\tau = \beta k_p \end{aligned} \quad (8)$$

where $p = 2\pi/\omega$. When $\phi(\omega) < \pi/2$, β is positive and the integral controller in Eq. (4) makes k_p be zero, the maximum point of $g(\bar{u})$, by adjusting $\bar{u}(t)$.

Detailed convergence proof can be found elsewhere [9,10].

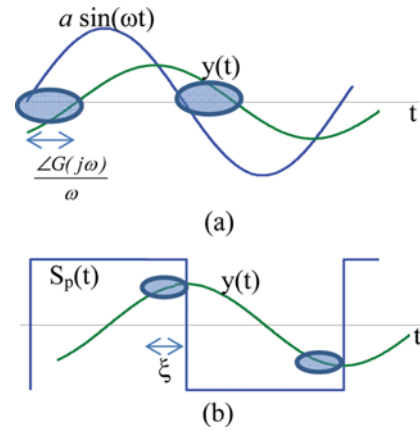


Fig. 2. Typical responses for sinusoidal and square-wave perturbations.

PROPOSED EXTREMUM SEEKING CONTROL

In Eq. (8), β should be positive and large to find the optimum point rapidly. Over the period of $np \leq t \leq np + \phi(\omega)/\omega$, the integral becomes negative, i.e.,

$$\int_{np}^{np + \phi(\omega)/\omega} \sin(\omega \tau) \sin(\omega \tau - \phi(\omega)) d\tau < 0 \quad (9)$$

where n is an arbitrary integer, as is exhibited in Fig. 2(a). Consequently, β is decreased, and the perturbed output is not utilized fully. When the process dynamics is fast enough compared to the excitation $\sin(\omega t)$, $\phi(\omega)$ is small, and its effect on the integration can be neglected. To reduce this effect for non-negligible $\phi(\omega)$, we may use $\sin(\omega t - \varsigma)$ instead of $\sin(\omega t)$ for $q(t)$ of Eq. (4), where ς is a constant approximation of $\phi(\omega)$. When $\phi(\omega)$ varies with \bar{u} , effectiveness of this approximation is limited.

To improve this weakness of the original ES control method, we propose a new method where the bias input \bar{u} is updated at each periodic instant of np as

$$\begin{aligned} \bar{q}_n &= \frac{1}{\xi} \int_{np-p/2-\xi}^{np-p/2} y(t) dt - \frac{1}{\xi} \int_{np-\xi}^{np} y(t) dt \\ \bar{u} &= k_I \sum_n \bar{q}_n \end{aligned} \quad (10)$$

Here we use the square-wave excitation [13].

$$\begin{aligned} u &= \bar{u} + a S_p(t) \\ S_p(t) &= \begin{cases} 1, & np < t \leq np + p/2 \\ -1, & np + p/2 < t \leq (n+1)p \end{cases} \end{aligned} \quad (11)$$

The input is perturbed by imposing a periodic square signal on the bias input \bar{u} , and the same periodic square signal is multiplied to the output as illustrated in Fig. 2(b) and Fig. 3.

As shown in Fig. 2(b), ξ is a time interval over which $S_p(t)$ and $y(t)$ have the same sign. The first and second integrals in Eq. (10) are for the positive and negative parts of $S_p(t)$, respectively. We select the design parameter ξ according to the magnitude of measurement noise. When $y(t)$ is noise-free, we set $\xi = 0$ and use the point data of

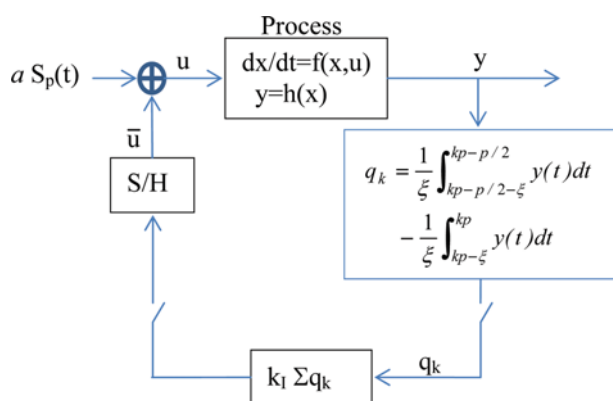


Fig. 3. Proposed extremum seeking control system.

$$\bar{q}_n = y(np - p/2) - y(np) \quad (12)$$

instead of the integrated values. With Eq. (12), the integral control will steer \bar{q}_n to zero, which corresponds to the state of $y(np - p/2) = y(np)$, or equivalently $k_p = 0$. When $y(t)$ is corrupted with noise, we increase ξ ($< p/2$) until noise is attenuated sufficiently through the integral in Eq. (10).

The singular perturbation technique is used to show stability of the extremum seeking control system, which consists of the fast dynamical process and the slow optimization [9,15]. With assuming $\dot{x} = f(x, u) = 0$ under that the process dynamics is fast enough, the slow subsystem becomes

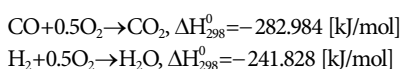
$$\begin{aligned} q_n &= g(\bar{u}_n + a) - g(\bar{u}_n - a) \\ \bar{u}_{n+1} &= \bar{u}_n + k_I q_n \end{aligned} \quad (13)$$

It is easy to show that this discrete-time system converges exponentially under mild assumptions of the steady state input-output relationship $g(u)$ of Eq. (2). The system of Eq. (13) acts as the slow manifold. The process of Eq. (1), which is assumed to be exponentially stable, acts as the boundary layer system. The singular perturbation can be used to show that interconnection of these two subsystems is also exponentially stable. Detailed stability proof finds assumptions on nonlinear functions in Eqs. (1) and (2). It is not investigated here because assumptions for stability are complicated and not very useful in the field applications.

SIMULATIONS

1. CO PROX Reactor

Hydrocarbon reforming can be used to produce hydrogen economically, a feed gas for the proton exchange membrane fuel cell. The hydrogen-rich gas from hydrocarbon reforming reactors can contain CO up to a several thousand ppm level, which poisons the anode catalyst of some fuel cells. The CO concentration needs to be removed below 10ppm. The preferential oxidation (PROX) is one of the simplest ways that can be employed for this purpose. In the reformer gas oxidation, the following two reactions compete:



where the CO oxidation should occur preferentially over the H_2

oxidation. The copper-cerium oxide catalyst of CuO-CeO_2 has been reported to have higher activity and selectivity for CO oxidation than for H_2 oxidation [17]. A packed bed reactor for CO PROX reactions has been reported in [18], and the dynamic model is given as

$$\begin{aligned} 600\dot{T}(t) &= -T(t) + 50.4 + 3.79u(t) \\ C_{\text{CO}}(t) &= 0.15272(T(t) - 160)^2 + 0.13534(T(t) - 160) + 2.4892 \\ y(t) &= 1 - \frac{C_{\text{CO}}(t - \theta)}{1000} \end{aligned} \quad (14)$$

Here T , C_{CO} , u , and y denote the reactor temperature in centigrade, the effluent concentration of CO in ppm, the heater control signal, and the CO conversion, respectively. The time delay θ represents an unknown delay, including the measurement delay. The CO conversion shows a maximum with $\bar{y}_{\text{opt}} = 0.9975$ at $\bar{T}_{\text{opt}} = 159.6^\circ\text{C}$. Under this condition, $\bar{C}_{\text{COopt}} = 2.459$ ppm. The dynamic model (14) shows input multiplicity, and hence a parallel compensator should be included to ensure global stability when conventional feedback controllers are applied [19].

The original and proposed ES control methods are applied to investigate and compare the extremum seeking performance. Parameters for the original ES controller were set at $p=100$ s ($\omega=0.0628$ s $^{-1}$), $a=0.2$, $k_f=0.3768$ s $^{-1}$, $\tau_H=159.2$ s, and $\tau_L=79.6$ s, respectively. Those for the proposed ES controller were given as $p=100$ s, $a=0.2$, $k_f=12.56$, and $\xi=10$ s.

Fig. 4 shows control responses for the CO PROX reactor under noise-free environments. For $\theta=0$, both original and proposed ES controllers succeed to find the optimal operation point, although convergence rates are different. When $\theta=6$ s, the original ES method fails to find the optimal point. On the other hand, the proposed ES controller succeeds in finding and maintaining the optimal point.

Fig. 5 shows control responses under noisy environments. Here the CO measurement is corrupted with uniform noise of ± 2 ppm. The measurement delay is set to $\theta=10$ s. The proposed ES controller with point data (Eq. (12)) shows somewhat irregular responses. On the other hand, the proposed ES controllers with $\xi=10$ s show

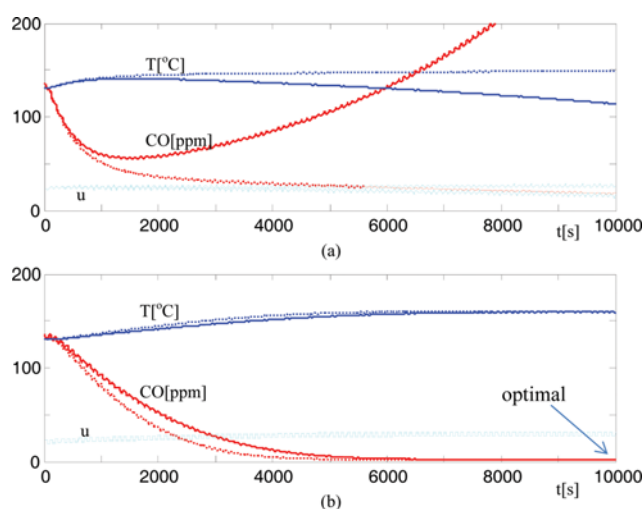


Fig. 4. Simulation results for the CO PROX Reactor system without noise (Solid line: $\theta=6$ s, Dotted line: $\theta=0$ s).

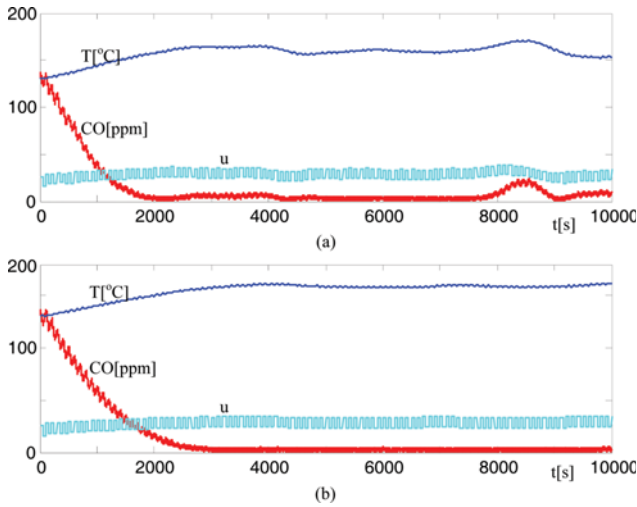


Fig. 5. Simulation results for the CO PROX Reactor system with noise ($\theta=10$ s, noise: uniform with ± 2 ppm in CO concentration).

excellent responses. The original ES controller fails to converge to the optimum point with the noisy measurement condition.

2. van de Vusse Reactor

Consider a continuous stirred tank reactor where the van de Vusse reactions occur [16,20].

$$\begin{aligned}\dot{x}_1 &= -k_{r1}x_1 - 2k_{r3}x_1^2 + (C_{Af} - x_1)u \\ \dot{x}_2 &= k_{r1}x_1 - k_{r2}x_2 - x_2u \\ y &= x_2\end{aligned}\quad (15)$$

The steady state values are

$$\begin{aligned}\bar{x}_1 &= \frac{-k_{r1} - \bar{u} + \sqrt{(k_{r1} + \bar{u})^2 + 8k_{r3}C_{Af}\bar{u}}}{4k_{r3}} \\ \bar{x}_2 &= \frac{k_{r1}\bar{x}_1}{k_{r2} + \bar{u}} = \bar{y}\end{aligned}\quad (16)$$

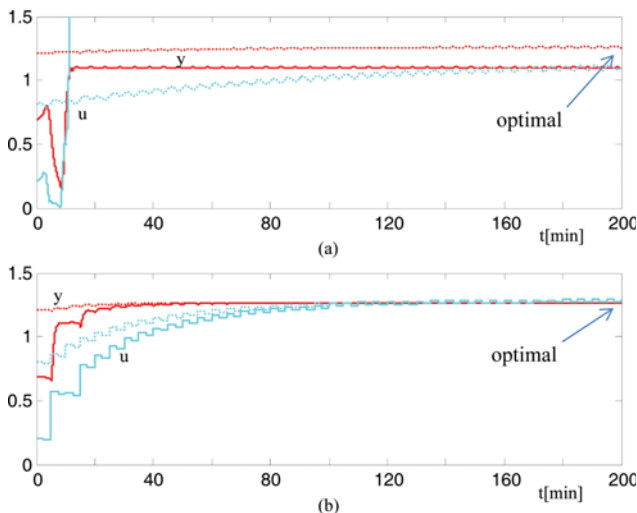


Fig. 6. Simulation results for the van de Vusse Reactor system from two different initial states ($p=5$ min) under noise-free environments.

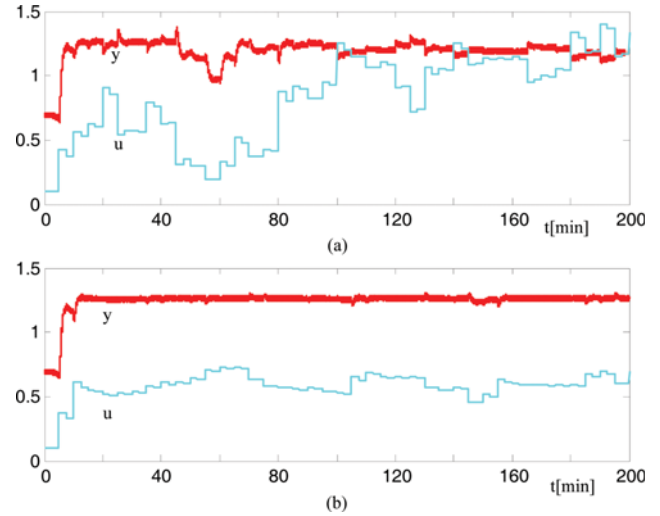


Fig. 7. Simulation results for the van de Vusse Reactor system with noise ($p=5$ min, noise: uniform with ± 0.02 in y).

Here, process parameters of $k_{r1}=5/6 \text{ min}^{-1}$, $k_{r2}=5/3 \text{ min}^{-1}$, $k_{r3}=1/12 \text{ L/(mol min)}$ and $C_{Af}=10 \text{ mol/L}$ are used. The optimal point is $\bar{u}_{opt}=1.292 \text{ min}^{-1}$ and $\bar{y}_{opt}=1.266 \text{ mol/L}$. Parameters for the original ES controller are set to $p=5 \text{ min}$ ($\omega=1.256 \text{ min}^{-1}$), $a=0.02$, $k_f=6.28 \text{ min}^{-1}$, $\tau_{H}=1.592 \text{ min}$ and $\tau_L=0.7962 \text{ min}$. Those for the proposed ES controller are set to $p=5 \text{ min}$, $a=0.01$, $\xi=0.1 \text{ min}$ and $k_f=3.768$.

Fig. 6 shows control responses for the van de Vusse reactor under noise-free environment. For an initial state of $\bar{u}=0.8$, both original and proposed ES controllers succeed to find the optimal operation point although convergence rates are different. For the initial state of $\bar{u}=0.2$, the original ES method fails to find the optimal point. However, the proposed ES controller succeeds in finding and maintaining the optimal point.

Fig. 7 shows control responses for the van de Vusse reactor under noisy environments. Here uniform noises of $\pm 0.02 \text{ mol/L}$ are added to the output y . The proposed ES controller with point data (Eq. (12)) is capable of reaching the optimum point, but shows irregu-

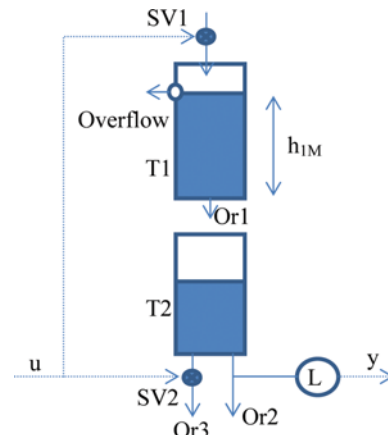


Fig. 8. Liquid level system (T1 and T2 are cylinders, SV1 and SV2 are solenoid valves, Or1, Or2 and Or3 are orifices, L is the level sensor).

lar responses. On the other hand, the proposed ES controller with $\xi=0.1$ min shows smooth and excellent responses.

3. Liquid Level System

Nonlinearities showing optimal points are often found in reaction processes as above. Those reaction processes are rather hard to construct and operate. As an easier system to test the ES controller experimentally, a liquid level system as shown in Fig. 8 is suggested. The system can be implemented to our BELL (bit evolutionary liquid level) system [21]. The mathematical model for the system in Fig. 8 can be written as follows:

$$\begin{aligned} A\dot{h}_1 &= \begin{cases} \beta u - a_1\sqrt{2gh_1}, & h_1 < h_{1M} \\ 0, & \text{otherwise} \end{cases} \\ A\dot{h}_2 &= a_1\sqrt{2gh_1} - a_2\sqrt{2gh_2} - a_3\sqrt{2gh_1}u \\ y &= h_2 \end{aligned} \quad (17)$$

where

A: cross-sectional area of tanks (19.625 cm^2)

h_1, h_2 : liquid levels of tanks [cm]

h_{1M} : overflow height in Tank 1 (25 cm)

a_1, a_2, a_3 : cross-sectional area of orifice tubes (0.0314 cm^2)

g: gravitational acceleration ($=980 \text{ cm/s}^2$)

β : a constant ($9.83 \text{ cm}^3/\text{s}$)

u: control input (pulse width modulation signal between 0 and 1)

y: process output (height of Tank 2)

The steady state input-output map is

$$\bar{y} = \begin{cases} \frac{\beta^2 \bar{u}^2}{2ga_2^2(1+a_3\bar{u}/a_2)^2} = 50 \frac{\bar{u}^2}{(1+\bar{u})^2}, & \text{if } \bar{u} < \frac{a_1\sqrt{2gh_{1M}}}{\beta} \\ \frac{a_1^2 h_{1M}}{(a_2+a_3\bar{u})^2} = \frac{25}{(1+\bar{u})^2}, & \text{otherwise} \end{cases} \quad (18)$$

The proposed ES controller is designed to have $p=400$ s, $a=0.002$ and $k_f=0.157$. Sampling time is set at 5 s. Noise-free cases with Eq. (12) are simulated. Two responses from initial steady state inputs

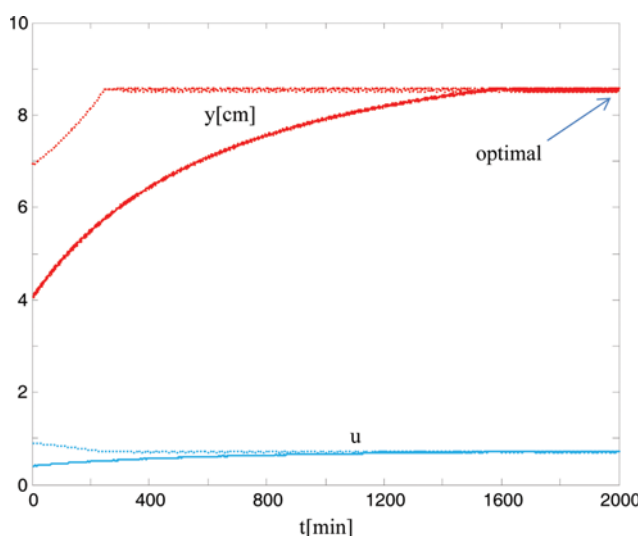


Fig. 9. Simulation results for the liquid level system.

\bar{u} of 0.4 and 0.9 are shown in Fig. 9. For both cases, the proposed ES controller drives the process to the optimal operating point of $\bar{u}_{opt}=0.707$ and $\bar{y}_{opt}=8.58$ cm. The original ES control fails to reach the optimal operating point with the perturbation signal of $\sin(\omega t)$, $\omega=2\pi/400 \text{ s}^{-1}$.

CONCLUSIONS

Extremum seeking (ES) control has been extensively studied as a promising method for the real-time optimization of processes. Although based on a static nonlinear process, it can be successfully applied to dynamic nonlinear processes. The ES controller uses a continuous perturbation and, for stability, time-scales among the process dynamics, the perturbation signal and the optimization rate should be separated. The perturbation signal should be slow enough, compared to the process dynamics. However, for some processes, fast perturbations are preferred because they can be attenuated easily in subsequent processes such as buffers and storages. For this, an ES control method that uses a square-wave perturbation and the partial sum of perturbation-output product is proposed. Compared to the original ES controller, a faster perturbation is allowed in the proposed ES controller. Simulations for two processes of parallel reactions have been given. In addition, a simple liquid level system to test ES control methods is also suggested.

ACKNOWLEDGEMENT

This work (2014004928) was supported by Mid-Career Research Program through NRF grant funded by the MEST.

REFERENCES

1. D. E. Seborg, T. F. Edgar, D. A. Mellichamp and F. J. Doyle, *Process dynamics and control*, 3rd Ed., Wiley, New York, U.S.A. (2010).
2. S. Skogestad, *J. Process Control*, **10**, 487 (2000).
3. C. Zhang and R. Ordonez, *Automatica*, **45**, 634 (2009).
4. S. Z. Khong, D. Nesic, C. Manzie and Y. Tan, *Automatica*, **49**, 1970 (2013).
5. K. S. Lee and W. K. Lee, *AIChE J.*, **31**, 667 (1985).
6. D. Nesic, A. Mohammadi and C. Manzie, *IEEE Trans. Automatic Control*, **58**, 435 (2013).
7. S. K. Korovin and V. I. Utkin, *Automatica*, **10**, 525 (1974).
8. L. Fu and U. Ozguner, *Automatica*, **47**, 2595 (2011).
9. M. Krstic and H. H. Wang, *Automatica*, **36**, 595 (2000).
10. Y. Tan, D. Nesic, I. M. Mareels and A. Astolfi, *Automatica*, **45**, 245 (2009).
11. Y. Tan, W. H. Moase, C. Manzie, D. Nesic and I. M. Mareels, *Proc. 29th Chinese Control Conference*, July 29-31, Beijing, China (2010).
12. M. Krstic, *Systems & Control Letters*, **39**, 313 (2000).
13. Y. Tan, D. Nesic and I. M. Mareels, *Automatica*, **44**, 1446 (2008).
14. A. Scheinker and M. Krstic, *Systems & Control Letters*, **63**, 25 (2014).
15. D. Dochain, M. Perrier and M. Guay, *Mathematics and Computers in Simulation*, **82**, 369 (2011).
16. M. Guay, *J. Process Control*, **24**, 98 (2014).
17. D. H. Kim, D. R. Park and J. Lee, *Int. J. Hydrogen Energy*, **38**, 4429 (2013).

- (2013).
18. H. C. Lee, S. Kim, J. P. Heo, D. H. Kim and J. Lee, *ADCHEM 2015*, Whistler, Canada (2015).
19. J. Lee and T. F. Edgar, *Korean J. Chem. Eng.*, **33**, 416 (2016).
20. B. W. Bequette, *Process dynamics modeling, analysis, and simulation*, Prentice Hall, New Jersey, U.S.A. (1998).
21. J. Lee, D. H. Kim, D. R. Yang and W. Cho, *AIChE Spring Meeting*, Austin, Texas, U.S.A. (2015).